Title
Size tunable three-dimensional annular laser trap based on axicons.

Journal
Optics Letters, 31(22)

ISSN
0146-9592

Authors
Shao, Bing
Esener, Sadik C
Nascimento, Jaclyn M
et al.

Publication Date
2006-11-15

DOI
10.1364/ol.31.003375

Size tunable three-dimensional annular laser trap based on axicons

Bing Shao and Sadik C. Esener

Department of Electrical and Computer Engineering, University of California, San Diego, La Jolla, California 92093

Jaclyn M. Nascimento and Michael W. Berns

Department of Bioengineering, University of California, San Diego, La Jolla, California 92093

Elliot L. Botvinick

Department of Biomedical Engineering, Beckman Laser Institute, University of California, Irvine, Irvine, California 92612

Mihrimah Ozkan

Department of Electrical Engineering, University of California, Riverside, Riverside, California 92521

Received July 11, 2006; revised August 16, 2006; accepted September 5, 2006; posted September 8, 2006 (Doc. ID 72842); published October 26, 2006

A three-dimensional (3D) ring-shaped laser trap has been built using axicons. The diameter of this laser trap ranges from 70 to 140 μm and is adjusted by simply changing the position of one axicon in the optical path. Parallel 3D trapping of 5 μm silica microspheres and 3D confinement of cells along the ring are demonstrated. In this system the special optical properties of axicons are used to create a continuous annular trap with high power efficiency and a constant numerical aperture. This new approach, without any mechanical scanning, offers significant potential for applications in cell motility analysis and biotropism studies.

OCIS codes: 140.7010, 170.4520, 220.4830.

Near-infrared laser trapping is a noninvasive tool that has been widely applied to manipulate biological cells[1,2] and organelles.[3] Since the late 1980s, calibrated optical traps have been used to measure physical forces in biological systems. One example is animal fertility, where researchers have been using laser tweezers to trap an individual sperm and quantitatively evaluate its swimming force.[4,5] As a result, the relationship between sperm motility and swimming pattern was studied,[5] and biomedical aspects of sperm activity were investigated.[6,7] Nevertheless, single-spot laser trapping analyzes one sperm at a time, lacks the ability of *in situ* sorting based on motility, and has difficulty in assessing the role of chemotaxis—a critical feature of sperm that is important in infertility and contraceptive approaches.[8]

An optical element with a conical surface that was introduced by McLeod[9,10] half a century ago, the axicon has been used to generate ring-shaped intensity profiles for laser machining[11] and atom trapping[12] and to generate nondiffracting Bessel beams for axial aligning, guiding, and stacking particles.[13] In this Letter we introduce a new type of optical trapping based on axicons that can be used to manipulate tens to hundreds of microparticles in parallel. This capability shows promise for high-throughput, multilevel sorting of self-propelled cells such as sperm. One advantage of a ring trap over a line trap is its ability to provide an equal-distance (from the center) condition that is important for biotropism studies. When an attractant is fixed in the center of the ring, the laser power or ring diameter can be adjusted so that only cells swimming with sufficient energy and sensitivity to the attractant's local concentration gradient have enough energy to overcome the trap and reach the attractant. In addition, a ring trap provides a way to confine a swimming cell in the field of view for an extended period of time without having to deal with sharp turns and changes in swimming curvature. The optical gradient force in the radial direction can guide a sperm along the ring. As a result, the effect of the laser on cells can be studied by monitoring changes in membrane potential (with a fluorescent probe) or motility. We expect that this new form of optical trapping will benefit a variety of cell motility and biotropism studies.

Compared with other methods for creating an annular trap, such as generalized phase contrast that needs counterpropagating beams for 3D confinement,[14] holographic optical trapping that generally suffers from low diffraction efficiency and needs a high-resolution spatial light modulator,[15] our system offers 3D trapping with almost 100% power efficiency. In addition, it is free from mechanical scanning, which introduces a tangential drag force to the sample.[16]

The experimental setup is depicted in Fig. 1. The light beam from a cw ytterbium fiber laser with a 1070 nm wavelength is collimated and expanded via the beam expander. When this Gaussian beam is incident on the axicon, an asymmetrical intensity pattern (half-Gaussian) from each azimuthal angle will be generated. According to the Fourier transform, this leads to a tilted phase front at the specimen plane, indicating that the total photon momentum transfer is not perpendicular to the specimen plane, and the stability of the trap is degraded.[17] For better trapping performance, a refractive beam shaper is

0146-9592/06/223375-3/$15.00

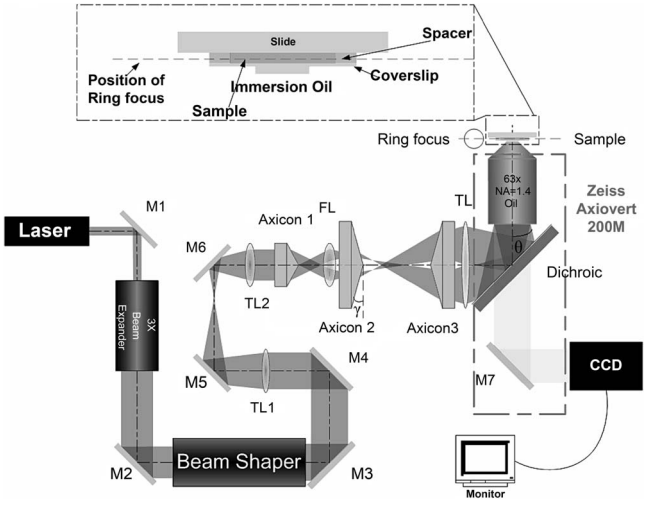

Fig. 1. Experimental setup of the dynamically adjustable annular laser trap. M1–M7, mirrors.

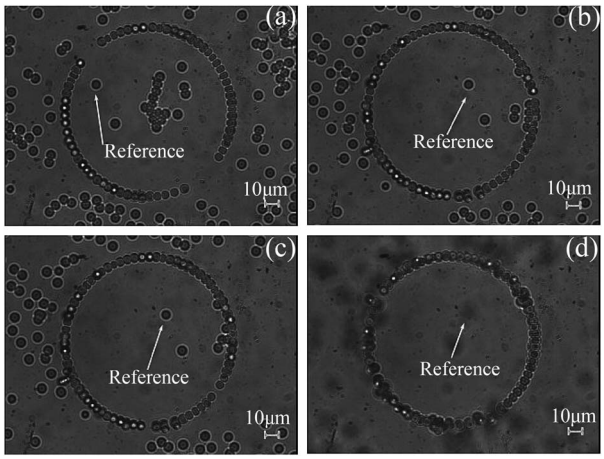

Fig. 2. Sequences of video frames showing (a), (b) a ring of trapped 5 μm silica beads being moved in the transverse direction and then (c), (d) being lifted 100 μm in the axial direction.

used to convert the Gaussian beam into a collimated flattop beam. A telescope lens pair (TL1, TL2) shrinks the beam so that the thickness of the light cone input to the objective is equal to the diameter of the back aperture, maximizing the numerical aperture of the trapping beam.[2] At axicon 1 ($\gamma=10°$) the input beam is divided with respect to the optical axis and bent toward it at an angle $\beta=\arcsin(n\sin\gamma)-\gamma=5.16°$, where γ is the base angle and n is the refractive index of the axicon. At the back focal plane of the focusing lens (FL), a ring image is formed that is conjugated to the ring focus at the specimen plane. After the tube lens (TL) the laser light is sent into an inverted microscope via a dichroic mirror whose reflecting surface faces the side. As a result, side-input light is directed upward into the objective.

The size of the ring trap is determined by the apex angle of the input light cone (θ in Fig. 1). To change θ while keeping the objective back aperture completely filled, axicons 2 and 3 ($\gamma=20°$) are added. The ability of an axicon to bend light without changing its collimation degree makes an axicon pair a better choice than a normal telescope lens pair.

Here 5 μm diameter silica microspheres are used to evaluate the performance of the annular trap. A microsphere–water suspension is put into a 120 μm thick chamber with a glass slide as the top and a no. 1 coverslip as the bottom. The lateral trapping force is determined by moving the stage and measuring the escape velocity of the trapped bead, and the axial trapping ability is verified by adjusting the height of the objective. Assuming spherical object symmetry and laminar fluid flow, the fluidic drag on an object is determined from the Navier–Stokes equation. At the escape velocity, v_e, the optical trapping force is equal to the fluidic drag force such that $F_{\text{opt}}=F_{\text{drag}}=6\pi\eta r v_e$,[18,19] where $\eta=1\times10^{-3}$ N S m^{-2} for water and r is the radius of the particle.

With an estimated trapping power of 23 mW per microsphere, a lateral trapping force of 8.14 pN could be obtained, and particles can stay trapped as the objective is moved in the axial direction at an average speed of 8 μm/s. Figure 2 shows the 3D trapping of 5 μm silica microspheres with a 63× oil immersion objective (NA=1.4). Figures 2(a) and 2(b) correspond to two different x positions of the stage, demonstrating the confinement of particles along the circumference of the ring. Figures 2(c) and 2(d) depict the lifting of trapped particles while the height of the objective is adjusted.

The geometrical structure of the ring trap is experimentally shown by moving the objective in the axial direction. In Fig. 3(a), when the image plane of

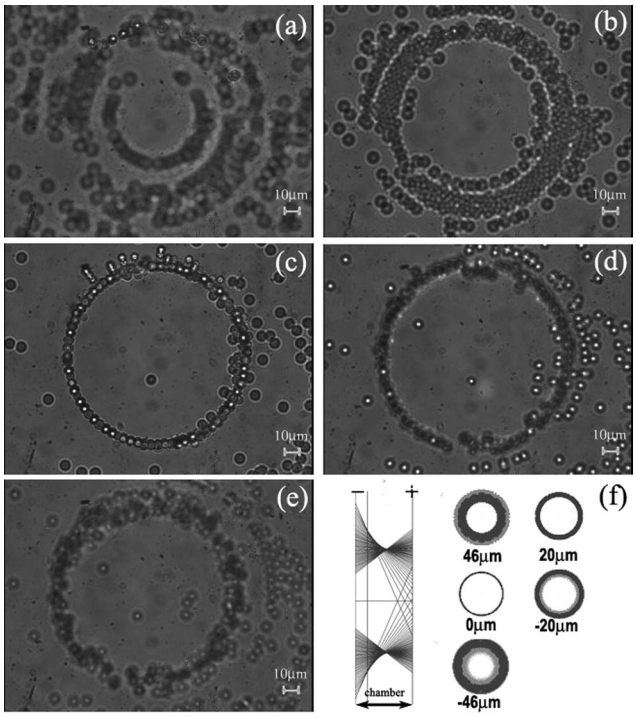

Fig. 3. Geometrical structure of the annular trap: experiment and simulation. (a) Objective height $z=46$ μm, (b) 20 μm, (c) 0 μm, (d) −20 μm, and (e) −46 μm. (f) ZEMAX simulation. Left, the cross section of light rays in the chamber when $z=0$ μm; right, the spot diagrams at the center of the chamber when the objective is at different heights corresponding to (a)–(e).

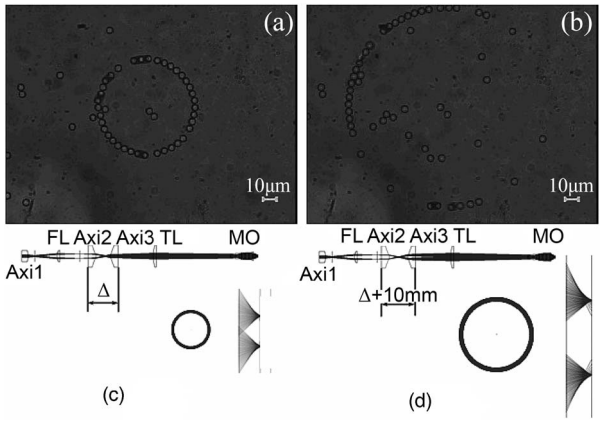

Fig. 4. Size tunability. (a) At the original axial position of axicon (Axi) 2, the diameter of the ring trap is 70 μm. (b) When axicon 2 is shifted to the left for 10 mm, the ring diameter increases to 140 μm. (c), (d). ZEMAX simulated layout, focus closeup, and sample plane spot diagram for (a) and (b). MO, microscope objective.

the objective is 46 μm above the center of the chamber, the ring focus is close to the ceiling and particles in the center of the chamber are arranged into concentric rings. As the objective is lowered [Fig. 3(b)], the ring focus is closer to the center of the chamber, and the concentric rings of particles have smaller radial spacings. When the ring focus arrives at the center of the chamber, particles are attracted to a single ring [Fig. 3(c)]. Further lowering the objective makes concentric rings of particles appear again in the center of the chamber. The lower the objective, the larger the spacing becomes between the rings [Figs. 3(d) and 3(e)]. These observations agree with ZEMAX simulation with a comparable objective[20] in Fig. 3(f), which shows the localization of the ring focus.

The size variable annular trap is demonstrated with 5 μm microspheres. Figure 4 shows that moving axicon 2 an additional 10 mm away from axicon 3 increased the diameter of the ring from 70 μm [Figs. 4(a) and 4(c)] to 140 μm [Figs. 4(b) and 4(d)]. This ensures the system's flexibility for trapping particles with different sizes and makes it easy to adjust the throughput. Besides microspheres, biological cells including red blood cells and self-propelled sperm can also be trapped in three dimensions.[17]

We have presented a new type of axicon trapping that allows parallel 3D manipulation of microparticles. This system has potential applications for motility and biotropism studies on self-propelled cells.[17] In our system the special optical properties of axicons are used to create a continuous, variable size annular trap with high power efficiency and constant numerical aperture. Experiments with microspheres and biological cells have proved the performance of the annular traps and their applicability to both inorganic and organic microparticles.

This work was supported by the Scripps Institute of Oceanography, and the Beckman Laser Institute, Inc., foundation. We thank IGO Medical Group for providing human semen samples. B. Shao's e-mail address is bshao@soliton.ucsd.edu.

References

1. M. Ozkan, M. M. Wang, C. Ozkan, R. A. Flynn, and S. Esener, Biomed. Microdevices **5**, 47 (2003).
2. B. Shao, S. Zlatanovic, and S. C. Esener, in Proc. SPIE **5514**, 62 (2004).
3. M. W. Berns, Sci. Am. (Int. Ed.) **278**, 52 (1998).
4. W. H. W. Y. Tadir, O. Vafa, T. Ord, R. H. Asch, and M. W. Berns, Fertil. Steril. **52**, 870 (1989).
5. W. H. W. Y. Tadir, O. Vafa, T. Ord, R. H. Asch, and M. W. Berns, Fertil. Steril. **53**, 944 (1990).
6. Y. L. P. Patrizio, G. J. Sonek, M. W. Berns, and Y. Tadir, J. Androl **21**, 753 (2000).
7. E. A. Z. N. Dantas, Jr., Y. Tadir, M. W. Berns, M. J. Schell, and S. C. Stone, Fertil. Steril. **63**, 185 (1995).
8. M. Eisenbach and I. Tur-Kaspa, BioEssays **21**, 203 (1999).
9. J. H. McLeod, J. Opt. Soc. Am. **44**, 592 (1954).
10. J. H. McLeod, J. Opt. Soc. Am. **50**, 166 (1960).
11. R. T. M. Rious and P. A. Belanger, Appl. Opt. **17**, 1532 (1978).
12. Y. B. O. I. Manek and R. Grimm, Opt. Commun. **147**, 67 (1998).
13. V. G.-C. J. Arlt, W. Sibbett, and K. Dholakia, Opt. Commun. **197**, 239 (2001).
14. P. J. Rodrigo, V. R. Daria, and J. Gluckstad, Opt. Lett. **29**, 2270 (2004).
15. A. Lafong, W. J. Hossack, and J. Arlt, Opt. Express **14**, 3065 (2006).
16. M. M. Wang, C. A. Schnabel, M. Chachisvilis, R. Yang, M. J. Paliotti, L. A. Simons, L. McMullin, N. Hagen, K. Lykstad, E. Tu, L. M. Pestana, S. Sur, H. Zhang, W. F. Butler, I. Kariv, and P. J. Marchand, Appl. Opt. **42**, 5765 (2003).
17. B. Shao, "Applying optical forces and elastic light scattering for manipulation and analysis of biological optics," Ph.D. dissertation (University of California, San Diego, San Diego, 2006).
18. G. K. Batchelor, *An Introduction to Fluid Dynamics* (Cambridge U. Press, 1991).
19. S. R. B. S. P. Smith, A. L. Brody, B. L. Brown, E. K. Boyda, and M. Prentiss, Am. J. Phys. **67**, 26 (1999).
20. N. Furutake, "Immersion microscope objective lens system," U.S. patent 5,982,559 (November 9, 1999).